Available online at www.sciencedirect.com
SCIENCE DIRECT®
ELSEVIER
International Journal of Solids and Structures 42 (2005) 5848–5871
INTERNATIONAL JOURNAL OF SOLIDS and STRUCTURES
www.elsevier.com/locate/ijsolstr

Benchmark case studies in structural design optimization using the force method

R. Sedaghati *

Department of Mechanical and Industrial Engineering, Concordia University, 1455 de Maisonneuve Blvd. West, Montreal, Que., Canada H3G 1M8

Received 28 October 2004
Available online 14 April 2005

Abstract

A structural optimization algorithm is developed for truss and beam structures under stress–displacement or frequency constraints. The algorithm combines the mathematical programming based on the Sequential Quadratic Programming (SQP) technique and the finite element technique based on the Integrated Force Method. A new approach based on the single value decomposition technique has been developed to derive the compatibility matrix required in the force method. Benchmark case studies illustrate the procedure and allow the results obtained to be compared with those reported in the literature. It is shown that the computational effort required by the force method is significantly lower than that of the displacement method and in some cases such as structural optimization problems with multiple frequency constraints, the analysis procedure (force or displacement method) significantly affects the final optimum design and the structural optimization based on the force method may result in a lighter design.

Keywords: Structural design; Optimization; Finite element force method

1. Introduction

Equilibrium equations combined with the compatibility conditions are generally fundamental to analysis methods in structural mechanics. The equilibrium equations are basically balance of elemental forces. For statically determinate structures, it is well known that the equilibrium equations alone, expressed in terms of forces, are adequate to calculate unknown elemental forces. However, equilibrium equations are not sufficient to solve general structural analysis problems, as they have to be augmented by the compatibility

* Tel.: +1 514 848 7971; fax: +1 514 848 8635.
E-mail address: sedagha@alcor.concordia.ca

0020-7683/$ - see front matter
doi:10.1016/j.ijsolstr.2005.03.030

conditions. In other words, equilibrium equations are indeterminate in nature, and determinacy for a continuum is achieved by adding the compatibility conditions. If the equilibrium equations are written in terms of nodal displacements, the compatibility conditions can be indirectly satisfied and the number of equations and the displacement unknowns are identical. This is basically the essence of displacement method.

A structure in the force method of analysis can be designated as structure (n, m), where (n, m) are the force and displacement degrees of freedoms (*fof*, *dof*), respectively. The n component force vector $\mathbf{F}$ must satisfy the m equilibrium equations along with $r = (n - m)$ compatibility conditions. If $n = m$, the structure is determinate and its analysis is trivial, i.e. the equilibrium equations are sufficient to find the element forces. The emphasis here is on the analysis of indeterminate structure for which $n > m$. There are at present two main force formulations, the Classical Force Method (CFM) and the Integrated Force Method (IFM). Both the CFM and IFM use the same equilibrium equations. The equilibrium matrix is a $(m \times n)$ banded rectangular matrix, which is independent of the material properties and design parameters of the indeterminate structure (n, m). The equilibrium matrix can be easily assembled from elemental equilibrium matrices using the finite element analysis. In CFM first equilibrium equation is satisfied and then using compatibility conditions, the r redundant forces will be obtained. In the Classical Force Method, the compatibility conditions are generated by splitting the structure (n, m) into a determinate basis structure (m, m) and r redundant members. The compatibility conditions are written in the redundant members by establishing the continuity of deformations between the r redundant members and the basis structure (m, m) for the external loads, thus the redundant members are the primal variables of the compatibility conditions in the CFM. This procedure was originally developed by Navier (Timoshenko, 1953) for the analysis of indeterminate trusses.

Patnaik (1986) and Patnaik et al. (1991) developed the IFM method. In IFM, the compatibility matrix is obtained by extending St. Venant's principle of elasticity strain formulation to discrete structural mechanics (Patnaik and Joseph, 1986). Both equilibrium equations and compatibility conditions are satisfied simultaneously. The compatibility conditions are generated without any recourse to redundant members and the basis determinate structure.

Structural analysis and optimization algorithms developed in recent years have generally been based on the displacement method(Venkayya, 1978; Canfield et al., 1988; Mohr, 1992; Mohr, 1994; Flurry and Schmit, 1980; Haftka and Gurdal, 1992). Commercial finite element programs are based on the displacement method and very few investigations have been reported in structural optimization using the finite element force method. In the present study, the linear analysis based on the Integrated Force Method has been used to analyze and optimize the truss and beam structures under stress, displacement and frequency constraints. It is intended to investigate the efficiency of the force method in the structural optimization of the truss and beam structures, under displacement, stress and frequency constraints, by solving the equilibrium and compatibility equations simultaneously. A direct method has been used to generate the compatibility matrix for indeterminate structures, which, is based on the displacement–deformation relationship and the Singular Value Decomposition (SVD) technique without the need to select the consistent redundant members. The equilibrium matrix is also generated automatically through the finite element analysis.

In most recent works, reported in literatures, the optimization algorithms were mainly based on the optimality criterion technique because of its computational efficiency. For example Saka (1984), Khan (1984), Khot (1984), Venkayya and Tischler (1983), Grandhi and Venkayya (1988), Konzelman (1986), Khan and Willmert (1981), McGee and Phan (1991), Khot and Kamat (1985), Saka and Ulker (1992), and Sedaghati and Tabarrok (2000) employed optimality criteria methods in minimization of the weight of truss and beam structures under stress, displacement, frequency or stability constraints. Modern optimality criterion algorithms would involve the case of satisfying the multiple constraints (scaling) and Karush–Kuhn–Tuker (KKT) condition (resizing) alternatively. However when the cross-sectional area and principal moment of inertia are nonlinearly related (frame structures), the scaling procedures, normally used in the optimality criterion methods, are approximate in nature and the scaling itself needs an iteration procedure. In this

study the powerful nonlinear mathematical programming method, based on the Sequential Quadratic Programming (SQP) technique, has been utilized as the optimization algorithm to find the true optimum solution and the results have been compared with those obtained using optimality criterion technique.

The application and efficiency of the proposed methodology is illustrated by minimizing the weight of different benchmark truss and beam structures under displacement, stress and frequency constraints. It is shown that by using either the force or displacement method, as an analyzer does not affect the final optimum solutions of the problems with stress and displacement constraints. However, the force method is more computationally efficient than the displacement method. Moreover it has been demonstrated that using force or displacement method as an analyzer may affect the final optimum solution in the problems under multiple frequency constraints and the force method may cause lighter design. Finally it is found that using Sequential Quadratic Programming method as the optimiser may result lighter design in comparison to the optimality criterion technique commonly used in the literature.

In the following sections, a short description of the structural analysis using the force method is presented and subsequently the optimization algorithm is explained. Finally, the application of the algorithm is illustrated by structural optimizing of different benchmark case studies.

2. Structural analysis using the force method

A discrete finite element structure with m and n displacement and force degrees of freedom, respectively has m equilibrium equations and $r = n - m$ compatibility conditions. In static problems the equilibrium equations in the displacement formulation can be written as

$$\boldsymbol{K}\mathbf{U} = \mathbf{P} \tag{1}$$

where $\boldsymbol{K}$ is the system stiffness matrix of the structure (obtained by assembling the stiffness matrices of the individual elements), $\mathbf{U}$ is the nodal displacement vector and $\mathbf{P}$ is the external applied load vector. The compatibility conditions have been satisfied implicitly during the generation of Eq. (1). The equivalent form of Eq. (1) in the integrated force formulation can be written as (Patnaik, 1986; Patnaik et al., 1991)

$$\boldsymbol{S}\mathbf{F} = \mathbf{P}^* \tag{2}$$

where $\mathbf{F}$ is the element force vector. The matrix $\boldsymbol{S}$ and vector $\mathbf{P}^*$ can be obtained through the combination of the m equilibrium equations as

$$\boldsymbol{Q}\mathbf{F} = \mathbf{P} \tag{3}$$

and r compatibility equations as

$$\boldsymbol{C}\boldsymbol{\Delta} = \mathbf{0} \tag{4}$$

where the element deformation vector $\boldsymbol{\Delta}$ can be related to the element force vector $\mathbf{F}$ in accordance to

$$\boldsymbol{\Delta} = \boldsymbol{G}\mathbf{F} \tag{5}$$

thus

$$\boldsymbol{S} = \begin{bmatrix} \boldsymbol{Q} \\ \cdots \\ \boldsymbol{C} \quad \boldsymbol{G} \end{bmatrix}, \quad \mathbf{P}^* = \begin{bmatrix} \mathbf{P} \\ \cdots \\ \mathbf{0} \end{bmatrix} \tag{6}$$

where $\boldsymbol{Q}$, $\boldsymbol{C}$ and $\boldsymbol{G}$ are the $(m \times n)$ equilibrium matrix, $(r \times n)$ compatibility matrix and the $(n \times n)$ flexibility matrix, respectively. One should note that the matrices $\boldsymbol{Q}$, $\boldsymbol{C}$ and $\boldsymbol{G}$ are banded and they have full-row ranks of m, r and n, respectively. The matrices $\boldsymbol{Q}$ and $\boldsymbol{C}$ also depend on the geometry of the structure and

therefore, are independent of the material properties. For a finite element idealization, the generation of the equilibrium matrix $\boldsymbol{Q}$ and the flexibility matrix $\boldsymbol{G}$ is straightforward and can be obtained automatically. However the automatic generation of the compatibility matrix $\boldsymbol{C}$ is a laborious task in the standard force method. Moreover, the generation of $\boldsymbol{C}$ in the Integrated Force Method is based on the elimination of the m displacement degrees of freedom from the n elemental deformations.

The displacement–deformation relationship for the discrete structures can be obtained by equating the internal strain energy and the external work and can be explained as

$$\boldsymbol{\Delta} = \boldsymbol{Q}^{\mathrm{T}}\mathbf{U} \tag{7}$$

Eq. (7) relates the n deformations to the $m$nodal displacement degrees of freedom and hence, the $r = n - m$ compatibility equations can be arrived through the elimination of the m nodal displacements from the n deformations. To obtain the compatibility matrix, one may express the nodal displacements in terms of the member deformations by using Eq. (7) as

$$\mathbf{U} = (\boldsymbol{Q}\boldsymbol{Q}^{\mathrm{T}})^{-1}\boldsymbol{Q}\boldsymbol{\Delta} = (\boldsymbol{Q}^{\mathrm{T}})^{\mathrm{pinv}}\boldsymbol{\Delta} \tag{8}$$

where the matrix $(\boldsymbol{Q}^{\mathrm{T}})^{\mathrm{pinv}}$ denotes the Moore–Penrose pseudo-inverse of $\boldsymbol{Q}^{\mathrm{T}}$. Considering Eqs. (7) and (8), we may have

$$\boldsymbol{B}\boldsymbol{\Delta} = \mathbf{0} \tag{9}$$

where

$$\boldsymbol{B} = [\boldsymbol{I}_n - \boldsymbol{Q}^{\mathrm{T}}(\boldsymbol{Q}^{\mathrm{T}})^{\mathrm{pinv}}] \tag{10}$$

where $\boldsymbol{I}_n$ is the $(n \times n)$ identity matrix. Eq. (9) is similar to the compatibility equations given by Eq. (4). However, the matrix $\boldsymbol{B}$ is a $(n \times n)$ matrix with rank of r inferring that the rows of matrix $\boldsymbol{B}$ are dependent on each other. In order to extract the $(r \times n)$ compatibility matrix $\boldsymbol{C}$ form the matrix $\boldsymbol{B}$, i.e. to reduce the matrix $\boldsymbol{B}$ to matrix $\boldsymbol{C}$, the Singular Value Decomposition (SVD) method has been employed (Golub and Van Loan, 1996). By applying the SVD method to $\boldsymbol{B}$, we obtain

$$\boldsymbol{B} = \boldsymbol{R}\boldsymbol{\Sigma}\boldsymbol{T}^{\mathrm{T}} \tag{11}$$

where $\boldsymbol{R}$ and $\boldsymbol{T}$ are the $(n \times n)$ orthogonal matrices and

$$\boldsymbol{\Sigma} = \begin{bmatrix} \boldsymbol{\Lambda} & \mathbf{0} \\ \mathbf{0} & \mathbf{0} \end{bmatrix}_{n \times n} \tag{12}$$

with $\boldsymbol{\Lambda} = \mathrm{diag}\{\, \xi_1 \quad \xi_2 \quad \cdots \quad \xi_r \,\}$, where $\xi_1 \geqslant \xi_2 \geqslant \cdots \geqslant \xi_r > 0$ are positive numbers. It follows that

$$\boldsymbol{B} = \boldsymbol{R}\begin{bmatrix} \boldsymbol{C} \\ \mathbf{0} \end{bmatrix} \tag{13}$$

Therefore the $(r \times n)$ compatibility matrix $\boldsymbol{C}$ can be represented by

$$\boldsymbol{C} = \boldsymbol{\Lambda}[\,\mathbf{T}_1 \quad \mathbf{T}_2 \quad \cdots \quad \mathbf{T}_i \quad \cdots \quad \mathbf{T}_r\,]^{\mathrm{T}} \tag{14}$$

where the vector $\mathbf{T}_i$ denotes the ith column of the matrix $\boldsymbol{T}$.

Although Eq. (7) is quite adequate to determine the element deformations using the nodal displacements, however it is not sufficient to obtain the nodal displacements using the element deformations or forces since the redundant structures are represented by the rectangular equilibrium matrix Q with no inverse. This implies that the compatibility equations should be merged with the equilibrium equations. For this reason, using $\boldsymbol{S}$ instead of $\boldsymbol{Q}$ in Eq. (7) and solving for the nodal displacements $\mathbf{U}$, we obtain

$$\mathbf{U} = \boldsymbol{J}\boldsymbol{\Delta} \quad \text{or} \quad \mathbf{U} = \boldsymbol{J}\boldsymbol{G}\mathbf{F} \tag{15}$$

where

$$\boldsymbol{J} = m \text{ rows of } \boldsymbol{S}^{-\mathrm{T}} \tag{16}$$

In frequency analysis problems, the equations of the motion in the displacement formulation can be written as

$$\boldsymbol{M}\ddot{\mathbf{U}} + \boldsymbol{K}\mathbf{U} = \mathbf{0} \tag{17}$$

where $\boldsymbol{M}$ is the stiffness matrix of system and $\ddot{\mathbf{U}}$ is acceleration vector. Considering Eq. (15) and noting that $\boldsymbol{K}\mathbf{U}$ in the displacement method is equivalent to $\boldsymbol{S}\mathbf{F}$ in the force method, Eq. (17) may be written as

$$\boldsymbol{M}^{*}\ddot{\mathbf{F}} + \boldsymbol{S}\mathbf{F} = \mathbf{0} \tag{18}$$

where

$$\boldsymbol{M}^{*} = \begin{bmatrix} \widetilde{\boldsymbol{M}} = \boldsymbol{MJG} \\ \cdots\cdots \\ \mathbf{0} \end{bmatrix} \tag{19}$$

Eq. (18) represents the frequency equation in the framework of the force formulation. In free vibration analysis, it is assumed that element forces are harmonics in time, $\mathbf{F} = \overline{\mathbf{F}}\sin(\omega t)$, where ω and $\overline{\mathbf{F}}$ are circular frequency and force mode shape, respectively. Considering this, Eq. (18) can be written as

$$\boldsymbol{S}\overline{\mathbf{F}} - \omega^{2}\boldsymbol{M}^{*}\overline{\mathbf{F}} = \mathbf{0} \tag{20}$$

The natural frequencies can be obtained easily from Eq. (20) by using an eigenvalue extraction algorithm. To overcome some computational difficulties during the analysis, the $(n \times n)$ system of equations expressed by Eq. (20) can be reduced to a $(m \times m)$ system by taking advantage of the null matrices. To obtain this, the matrices in Eq. (20) are partitioned into the redundant and basis determinate structure as

$$\begin{bmatrix} \boldsymbol{S}_{mm} & \boldsymbol{S}_{mr} \\ \boldsymbol{S}_{rm} & \boldsymbol{S}_{rr} \end{bmatrix} \begin{bmatrix} \overline{\mathbf{F}}_{m} \\ \overline{\mathbf{F}}_{r} \end{bmatrix} - \omega^{2} \begin{bmatrix} \widetilde{\boldsymbol{M}}_{mm} & \widetilde{\boldsymbol{M}}_{rr} \\ \cdots\cdots & \\ \mathbf{0} & \end{bmatrix} \begin{bmatrix} \overline{\mathbf{F}}_{m} \\ \overline{\mathbf{F}}_{r} \end{bmatrix} = \mathbf{0} \tag{21}$$

or

$$\begin{aligned} &\boldsymbol{S}_{mm}\overline{\mathbf{F}}_{m} + \boldsymbol{S}_{mr}\overline{\mathbf{F}}_{r} - \omega^{2}(\widetilde{\boldsymbol{M}}_{mm}\overline{\mathbf{F}}_{m} + \widetilde{\boldsymbol{M}}_{rr}\overline{\mathbf{F}}_{r}) = \mathbf{0} \\ &\boldsymbol{S}_{rm}\overline{\mathbf{F}}_{m} + \boldsymbol{S}_{rr}\overline{\mathbf{F}}_{r} = 0 \end{aligned} \tag{22}$$

Eliminating of $\mathbf{F}_r$ from the $(n \times n)$ system of equations in Eq. (22) results in the reduced $(m \times m)$ subsystem as

$$(\boldsymbol{S}_{mm} - \boldsymbol{S}_{mr}\boldsymbol{S}_{rr}^{-1}\boldsymbol{S}_{rm})\overline{\mathbf{F}}_{m} - \omega^{2}(\widetilde{\boldsymbol{M}}_{mm} - \widetilde{\boldsymbol{M}}_{rr}\boldsymbol{S}_{rr}^{-1}\boldsymbol{S}_{rm})\overline{\mathbf{F}}_{m} = \mathbf{0} \tag{23}$$

and

$$\overline{\mathbf{F}}_{r} = \boldsymbol{S}_{rr}^{-1}\boldsymbol{S}_{rm}\overline{\mathbf{F}}_{m} \tag{24}$$

The solution of the reduced eigenvalue problem expressed by Eq. (23) gives all the eigenvalues, whereas both Eqs. (23) and (24) are used to calculate the force eigenvectors. Once the force mode shapes are determined, the displacement mode shapes can be generated by using Eq. (15).

It is noted that the selection of the redundant members is not unique and there are multiple combinations of redundant and basis determinate structure for an indeterminate structure. However the redundant members should be selected so that the remaining determinate structure is not a mechanism. This consistent

set of redundant members will ensure the existence of the inverse of $\boldsymbol{S}_{rr}$. If the equilibrium equations in Eq. (3) is rewritten in the following form:

$$\boldsymbol{Q}_r\mathbf{F}_r + \boldsymbol{Q}_m\mathbf{F}_m = \mathbf{P} \tag{25}$$

the selection of the consistent set of redundant members and basis determinate structure is such that the rank of the matrix $\boldsymbol{Q}_m$ is equal to m. The violation of this condition makes the matrix $\boldsymbol{Q}_m$ singular. Here, a robust technique based on the Gauss elimination technique and work of Robinson (1965) has been developed and applied to automatically identify the consistent set of redundant members and basis determinate structure. The proposed technique is outlined as follows:

I. Augment the equilibrium matrix $\boldsymbol{Q}$ with the external load $\mathbf{P}$ as $[\,\boldsymbol{Q} \quad \mathbf{P}\,]$; II. Select one of the nonzero elements in the first row of the augmented matrix and divide all the elements in this row by this number; III. Multiply the first row by the coefficient of the corresponding element in the second row (if it is not zero) and subtracted from the second row; IV. Continue this procedure for each of the remaining rows; V. The column corresponding to that element has now a one in the first row and zeros in all other rows; VI. Repeat the same process from steps II through IV, in turn for the remaining rows until either all of the rows are exhausted or all of the remaining rows have all zeros as elements; VII. All the m unit columns are independent and they correspond to the basis determinate structure. The remaining columns correspond to the consistent redundant members.

As mentioned before, consistent redundant members selected are not unique since the redundancy is dependent on the order in which the equations are generated and by the selection of the nonzero element in each row when applying the Gaussian elimination procedure.

4. Optimization algorithm

The optimization problem for truss and beam type of structures can be defined mathematically as minimizing the structural mass represented as

$$\text{Min}\left\{M(\mathbf{A}) = \sum_{i=1}^{N_e} \rho_i L_i A_i\right\} \tag{26}$$

subject to the $(N_\sigma + N_U)$ stress and the displacement constraints (behaviour constraints)

$$\begin{aligned} g_i(\mathbf{A}) &= |\,\sigma_i/\bar{\sigma}_i\,| - 1 \leqslant 0 \quad i = 1,\ldots,N_\sigma \\ g_j(\mathbf{A}) &= |\,U_j/\overline{U}_j\,| - 1 \leqslant 0 \quad j = 1,\ldots,N_U \end{aligned} \tag{27}$$

or subject to N_ω natural frequency constraints (behavior constraints)

$$g_k(\mathbf{A}) = \tilde{\omega}_k^2 - \omega_k^2 \leqslant 0 \quad k = 1,2,3,\ldots,N_\omega \tag{28}$$

and the N_A side constraints on the design variables

$$\overline{A}_i - A_i \leqslant 0 \quad i = 1,2,3,\ldots,N_A \tag{29}$$

where ρ_i, A_i and L_i are the density, the cross-sectional area and the length of the ith element, respectively. M is the total mass of the structure and $\overline{A}_i$ is the lower limit on the ith design variable. Furthermore, σ_i, $\bar{\sigma}_i$ are the stresses in the ith element and its allowable limit value, respectively, and U_j, $\overline{U}_j$ are the constrained displacement on the jth degrees of freedom and its allowable limit value. ω_k and $\tilde{\omega}_k$ are the kth natural frequency and its specified value, respectively.

It should be pointed out that the analysis and optimization are two separate modules. The equilibrium and compatibility equations in the force method, Eq. (2), and the frequency equation, Eq. (21), are satisfied

directly during the finite element analysis (analysis module) and then the results are passed to the optimization module. Thus it is not necessary to take into account Eq. (2) or Eq. (21) as the equality constraints inside the optimization algorithm.

In this study, the Sequential Quadratic Programming (SQP) method has been applied to solve the optimization problem discussed above. The implementation of the SQP method was performed in MATLAB (Coleman et al., 1999). Based on the work done by Powell (1978), the method allows one to closely mimic the Newton's method for the constraint optimization just as it is done for the unconstraint optimization. SQP is indirectly based on the solution of the KKT conditions. Given the problem description in Eqs. (26)–(29), the principal idea is the formulation of a QP sub-problem based on a quadratic approximation of the Lagrangian function as follows:

$$\mathrm{Lag}(\mathbf{A},\lambda) = M(\mathbf{A}) + \sum_{i=1}^{N_t} \lambda_i \cdot g_i(\mathbf{A}) \tag{30}$$

where N_t is the total number of constraints. At each major iteration of the SQP method a QP sub-problem is solved. The solution to the QP sub-problem produces an estimate of the Lagrange multipliers, λ_i, and a search direction vector $\mathbf{d}^v$ in each iteration v, which is used to form a new iteration as

$$\mathbf{A}^{v+1} = \mathbf{A}^v + \alpha^v \mathbf{d}^v \tag{31}$$

The step length parameter α^v is determined through a one-dimensional minimization in order to produce a sufficient decrease in the merit function. At the end of the one-dimensional minimization, the Hessian of the Lagrangian, required for the solution of the next positive definite quadratic programming problem, is updated using the Broyden–Fletchet–Goldfarb–Shanno (BFGS) formula as

$$\boldsymbol{H}^{(v+1)} = \boldsymbol{H}^{(v)} + \frac{\mathbf{q}^{(v)}\mathbf{q}^{T(v)}}{\mathbf{q}^{T(v)}\boldsymbol{\delta}^v} - \frac{\boldsymbol{H}^{T(v)}\boldsymbol{\delta}^{(v)}\boldsymbol{\delta}^{T(v)}\boldsymbol{H}^{(v)}}{\mathbf{d}^{T(v)}\boldsymbol{H}^{(v)}\mathbf{d}^{(v)}} \tag{32}$$

where

$$\delta^v = \mathbf{A}^{v+1} - \mathbf{A}^v \tag{33}$$

$$\mathbf{q}^v = \nabla\mathrm{Lag}(\mathbf{A}^{v+1},\lambda^{v+1}) - \nabla\mathrm{Lag}(\mathbf{A}^v,\lambda^v) \tag{34}$$

and $\boldsymbol{H}$ is the approximation of the Hessian of 'Lag' at $\mathbf{A}^{v+1}$.

Powell (1978) recommends keeping the Hessian positive definite even though it may be positive indefinite at the solution point. To guarantee that the updated Hessian matrix $\boldsymbol{H}^{v+1}$ remains positive definite, he suggests replacing $\mathbf{q}^v$ by $\theta\mathbf{q}^v + (1-\theta)\boldsymbol{H}^v\delta^v$ where $\mathbf{q}^v$ is given by Eq. (34), and θ is determined by

$$\theta = \begin{cases} 1 & \text{if } \boldsymbol{\delta}^{Tv}\mathbf{q}^v \geqslant 0.2\boldsymbol{\delta}^{Tv}\boldsymbol{H}\boldsymbol{\delta}^v \\ \dfrac{0.8\boldsymbol{\delta}^{Tv}\boldsymbol{H}\boldsymbol{\delta}^v}{0.8\boldsymbol{\delta}^{Tv}\boldsymbol{H}\boldsymbol{\delta}^v - \boldsymbol{\delta}^{Tv}\mathbf{q}^v} & \text{if } \boldsymbol{\delta}^{Tv}\mathbf{q}^v < 0.2\boldsymbol{\delta}^{Tv}\boldsymbol{H}\boldsymbol{\delta}^v \end{cases} \tag{35}$$

It should be noted that the stress–displacement and frequency gradient functions, in Eqs. (27) and (28), are not both smooth and convex functions, thus the local optimum result may be achieved using the gradient-based algorithms such as the above SQP algorithm. In this study, several randomly generated initial points have been used for the SQP algorithm in order to make sure that the optimal solution is either a global solution or very close to the global solution.

5. Benchmark case studies

A brief description of the test cases are outlined in Table 1.

Table 1
Benchmark Case Studies on structural optimization under stress, displacement and frequency constraints

Young's modulus $E = 6.89 \times 10^{10}$ pa (10^7 psi),
Density ρ =2770 kg/m^3 (0.1 lbm/in^3)

Constraints: Stress, Displacement and Area:

Allowable stress ±172.37 Mpa (±25000 psi)
Vertical disp. on nodes 1–4= ±254 mm (±2 in)
Minimum area set at 64.52 mm^2 (0.1 in^2)

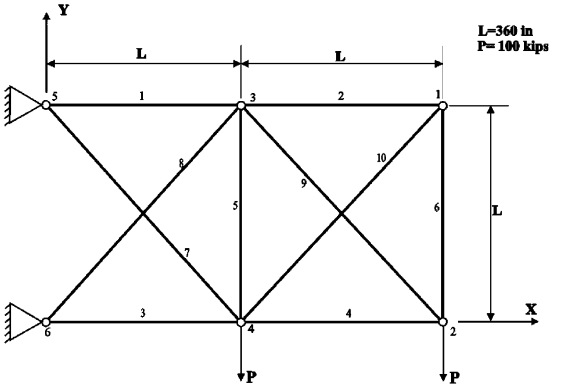

Fig. 1. The 10-bar planar truss structure.

Young's modulus $E = 2.07 \times 10^{11}$ KN/mm^2 (3×10^7 psi),
Density ρ =7830 kg/m^3 (0.283 lbm/in^3)

Constraints: Stress, Displacement and Area:

Allowable tension stress=240 Mpa (34809 psi)
Allowable compression stress=According to AISC code
Disp. on nodes 1 and 2=10 mm (0.039in^2) in X and Y dir.
Minimum area set at 200 mm^2 (0.31 in^2)

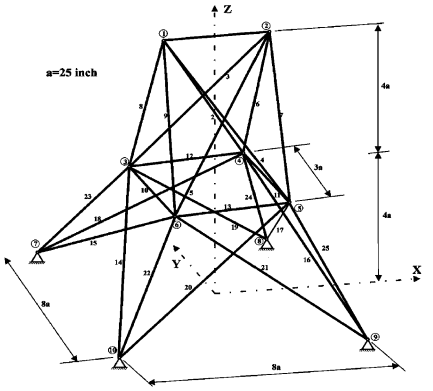

Fig. 2. The 25-bar space truss structure.

Young's modulus $E = 6.89 \times 10^{10}$ pa (10^7 psi),
Density ρ =2770 kg/m^3 (0.1 lbm/in^3)

Constraints: Stress, Displacement and Area:

Allowable stress = ±172.37 Mpa (±25 000 psi)
Disp. on nodes 1–4= ±6.35 mm (±0.25 in) in X and Y dir.
Minimum area set at 64.52 mm^2 (0.1 in^2)

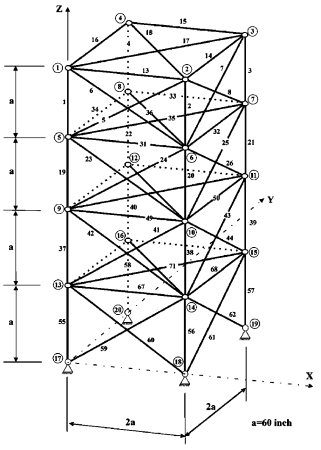

Fig. 3. The 72-bar space truss structure.

Young's modulus $E = 2.07 \times 10^{11}$ KN/mm^2 (3×10^7 psi),
Density ρ =7830 kg/m^3 (0.283 lbm/in^3)

Constraints: Stress, Displacement and Area:

Allowable stress= ±165.47 Mpa (24 000 psi)
Disp. on all nodes= 0.254 mm (0.01 in) in X dir.
Minimum area set at 3225.80 mm^2 (5 in^2)
Maximum area set at 64 516 mm^2 (100 in^2)

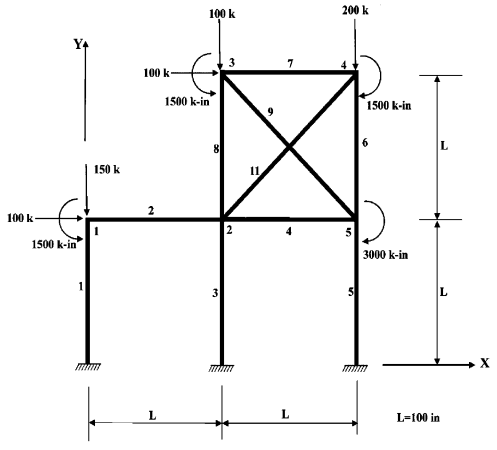

Fig. 4. 10-member frame.

(*continued on next page*)

Table 1 (*continued*)

Young's modulus $E = 2.07 \times 10^{11}$ KN/mm^2 (3×10^7 psi),
Density ρ =7830 kg/m^3 (0.283 lbm/in^3)

Constraints: Stress, Displacement and Area:

Allowable stress= ±165.47 Mpa (24 000 psi)
Disp. on nodes 1–3 and 10–12= 0.127 mm (0.005 in) in X dir.
Minimum area set at 3225.80 mm^2 (5 in^2)
Maximum area set at 64 516 mm^2 (100 in^2)

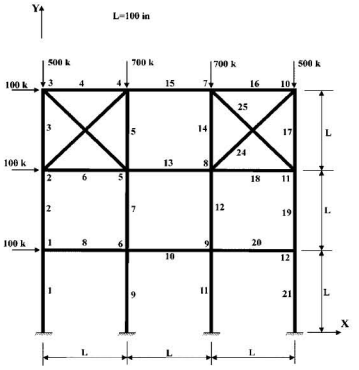

Fig. 5. 25-member frame.

Young's modulus $E = 6.89 \times 10^{10}$ pa (10^7 psi),
Density ρ =2770 kg/m^3 (0.1 lbm/in^3)
Lumped mass on nodes 1–4 m=454 kg (1000 lbm)

Constraints: Frequency and Area:

Fundamental Frequency $\omega_1 = 14$ Hz.
Second frequency ω_2 =25 Hz.
Multiple frequency: ω_1 =7, $\omega_2 \geqslant 15$, $\omega_3 \geqslant 20$ Hz
Minimum area set at 64.52 mm^2 (0.1 in^2)

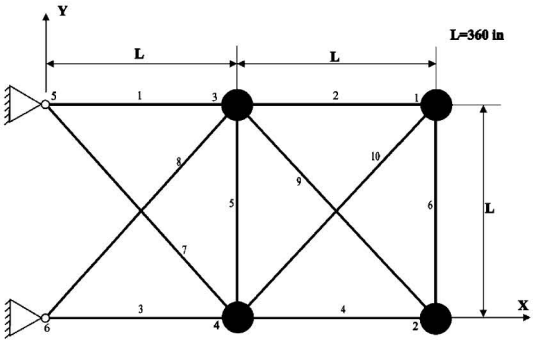

Fig. 6. 10-bar planar truss with lumped masses.

Young's modulus $E = 6.89 \times 10^{10}$ pa (10^7 psi),
Density ρ = 2770 kg/m^3 (0.1 lbm/in^3)
Lumped mass on nodes 1–4 m=2270 kg (5000 lbm)

Constraints: Frequency and Area:

Fundamental frequency $\omega_1 = 4$ Hz.
Multiple frequency: $\omega_1 = 4$, $\omega_3 \geqslant 6$ Hz
Minimum area set at 64.52 mm^2 (0.1 in^2)

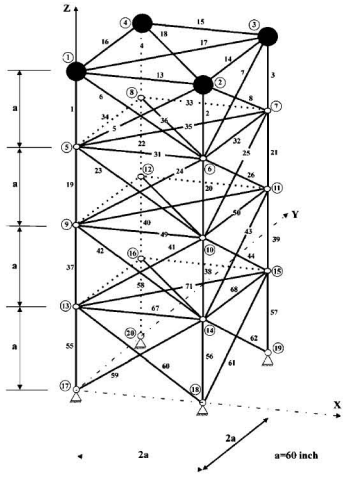

Fig. 7. 72-bar space truss with lumped masses.

Young's modulus $E = 2.07 \times 10^{11}$ KN/mm^2 (3×10^7 psi),
Density ρ = 7830 kg/m^3 (0.283 lbm/in^3)
Distributed nonstructural mass= 178.740 kg/m (10 lbm/in) on members 5 and 6.

Constraints: Frequency and Area:

Fundamental frequency $\omega_1 = 78.5$ Hz.
Multiple frequency: ω_1 =78.5, $\omega_2 \geqslant 180$ Hz
Minimum area set at 5108.8 mm^2 (7.9187 in^2)
Maximum area set at 56 955 mm^2 (88.28 in^2)

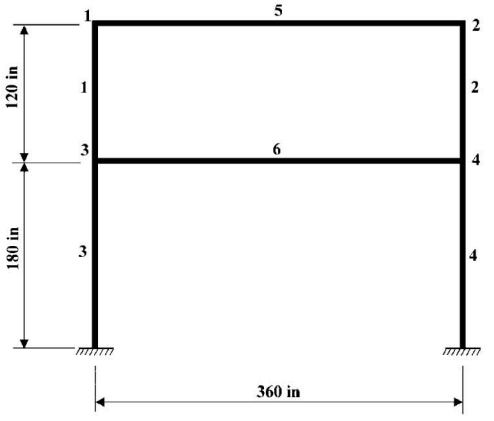

Fig. 8. 6-member frame with distributed nonstructural masses on members 5 and 6.

5.1. Stress and displacement constraints

Five examples on the analysis of the planar and space truss and frame structures shown in Figs. 1–5 (see Table 1) illustrate the proposed procedure and allow the results to be compared with those reported in literatures. All information regarding the material and geometrical characteristics, applied external loads, side constraints (minimum and maximum cross-sectional areas) and behaviour constraints (stress–displacement constraints) are provided in the relative figures. It is intended to show that in the structural optimization problems, with the stress and displacement constrains, the analysis procedure (either the force method or the displacement one) does not affect the final optimum design. Furthermore, it is to establish the fact that the design optimization procedure based on the force method is more efficient than the displacement method.

5.1.1. The 10-bar planar truss structure

The 10-bar planar truss is shown in Fig. 1 (see Table 1). This structural design problem is a classical example in the literature and has been extensively investigated using linear analysis based on the displacement method. The number of displacement degrees of freedom is $m = 8$ and the number of force degrees of freedom $n = 10$. Thus, the number of redundancy is $r = 2$.

A minimum mass of 2299.65 kg (5069.85 lbm) was obtained using both the displacement method (DM) and the force method (FM). The initial cross-sectional area for all the elements is 9677.4 mm^2 (15 $in.^2$), which is an infeasible guess. The horizontal negative displacement constraint at node 1 and the tension stress constraint in element 5 are active at optimum point. The final results are tabulated in Table 2. The iteration history is shown in Fig. 9. The CPU time required by the FM was significantly lower than the DM, thus confirming the efficiency of the FM. The cross-sectional areas in elements 2, 5 and 10 reached to their minimums in both analyses. It is interesting to note that both the stress constraint and the cross-sectional area are active in element 5. The results obtained match exactly the results reported by Flurry and Schmit (1980) and Haftka and Gurdal (1992), who solved the problem using the dual method and approximation concepts in linear analysis based on the displacement method.

Table 2
The final design solution for the cross-sectional areas ($in.^2$) for the 10-bar planar truss

Member	DM	FM
1	30.5218	30.5218
2	0.1000	0.1000
3	23.1999	23.1999
4	15.2229	15.2229
5	0.1000	0.1000
6	0.5514	0.5514
7	7.4572	7.4572
8	21.0364	21.0364
9	21.5284	21.5284
10	0.1000	0.1000
Mass (lbm)	5060.85	5060.85
No. of iterations	237	237
No. of A.C.[a]	5	5
CPU time (s)	11.24	4.34

[a] A.C.: Active Contraints.

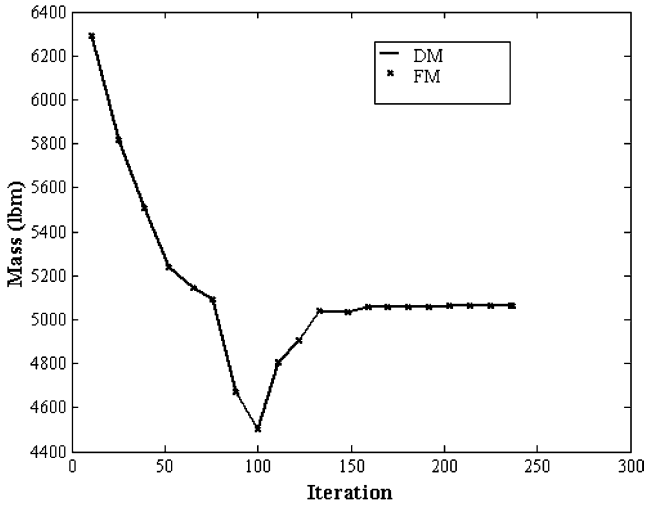

Fig. 9. Iteration history for the 10-bar planar truss using the force and displacement methods.

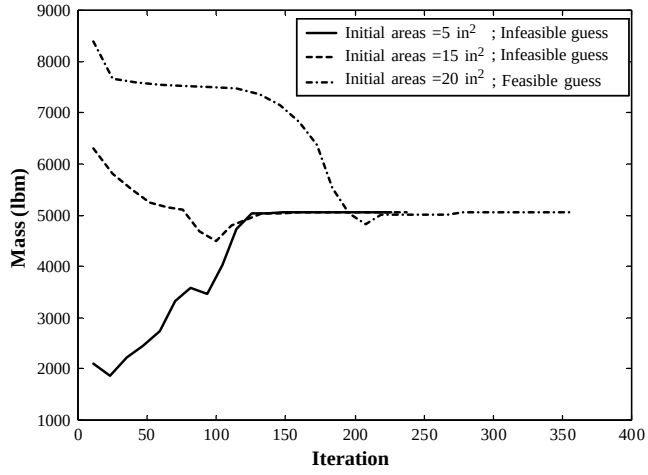

Fig. 10. Iteration history for different initial areas for the10-bar planar truss.

The problem was also solved using different initial cross-sectional areas for the elements. The results obtained were exactly the same as in the previous case. The iteration history for three different initial cross sectional areas (using the force method) is shown in Fig. 10.

5.1.2. The 25-bar space truss structure

The 25-bar space truss structure, shown in Fig. 2 (see Table 1), has previously been investigated by Saka using the linear analysis based on the displacement method and with the optimality criterion approach (Saka, 1984). The structure has identical symmetries about the X–Z and Y–Z planes, so that the design variable linking is used to impose symmetry on the structure and hence, only eight design variables are identified here. The structure is subjected to single load case as shown in Table 3.

Table 3
Nodal load components (N) for the 25-bar space truss structure

Node	Coordinate directions		
	X	Y	Z
1	80000	120000	30000
2	60000	100000	30000
3	30000	0	0
6	30000	0	0

The allowable compressive stress, σ_{ac}, is determined in accordance to the AISC codes (AISC, 1978) in which

$$\sigma_{ac} = \begin{cases} \pi^2 E/S_R^2 & \text{for } S_R > C_c \\ \sigma_{at}(1 - 0.5S_R^2/C_c^2) & \text{for } S_R < C_c \end{cases} \tag{36}$$

where the slender ratio of each member is $S_R = L/R_G$ (L is the length and R_G is the radius of gyration for each member) and $C_c = \sqrt{2\pi^2 E/\sigma_{at}}$ (σ_{at} is the allowable tension stress). Thus, the value of the allowable compressive stress varies during the optimization process. All the members have the pipe-type cross-sections with $S_R = aA^b$, where A is the cross-sectional area in square centimeter and the constants a and b are selected as 0.4993 and 0.6777, respectively. The number of degrees of freedom for the displacement is $m = 18$, and that of the force is $n = 25$. Therefore, the number of the redundancy is found to be $r = 7$. Without linking the design variables, the number of the design variables is 25 and, the number of the constraints is 54. On the other hand, by linking the design-variables into eight groups, the number of the design variables reduces to 8, and the number of the constraints would change to 20.

A minimum value of the mass of 649.7 kg (1432.3 lbm) was obtained using both the displacement method (DM) and the force method (FM). The final results for both displacement and force methods are presented in Table 4 with their iteration histories illustrated in Fig. 11. The initial cross-sectional area for all the elements is chosen as 2000 mm^2 (3.1 in.^{2}). The CPU time required for the FM is significantly lower than that of the DM indicating its superior efficiency. It ahs been realized that the compressive stress constraint in the elements 1, 2, 6, 10, 13, 16, 18 and 24 (one member from each group was selected) are found to be active.

Table 4
Final design solutions for the cross-sectional areas (mm^2) for the 25-bar space truss structure

Design variables	Member	DM	FM
1	1	232.7	232.7
2	2–5	1150.6	1150.6
3	6–9	895.1	895.1
4	10,11	230.4	230.4
5	12,13	223.3	223.3
6	14–17	1018.4	1018.4
7	18–21	950.2	950.2
8	22–25	1443.5	1443.5
Mass (kg)		649.7	649.7
No. of iterations		316	424
No. of A.C.[a]		8	8
CPU time (s)		50.64	16.31

[a] A.C.: Active Constraints.

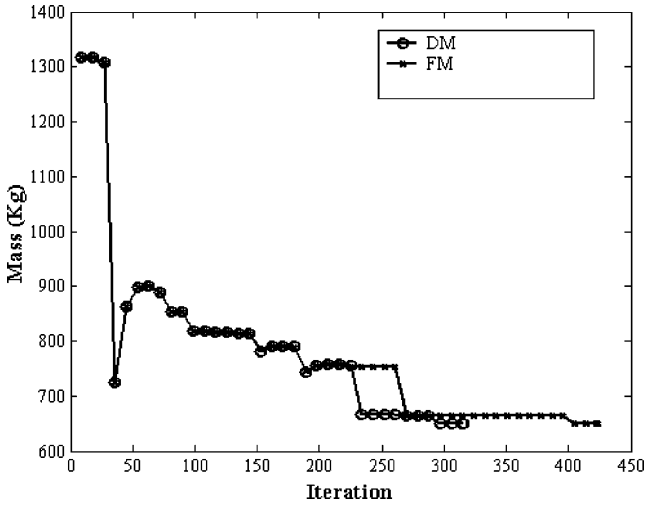

Fig. 11. Iteration histories for the 25-bar space truss structure using the displacement and force methods.

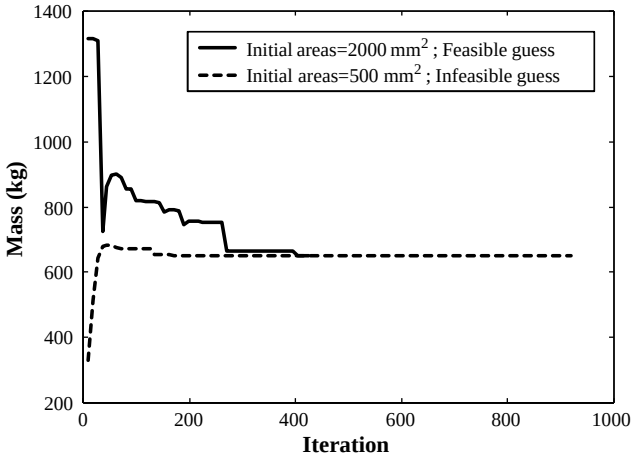

Fig. 12. Iteration histories for different initial areas for the 25-bar space truss.

To confirm that the global optimum has been caught, the problem was again solved, using different initial values of the cross-sectional areas for all the elements, and results were found to be exactly the same as for the previous case. The iteration histories for two different initial values of the cross-sectional area, using the force method, is shown in Fig. 12.

A minimum value of the weight of 921 kg (2030.5 lbm) has been reported obtained by Saka, using the displacement method combined with the optimality criterion based only on satisfying the displacement constraints (Saka, 1984). The stress constraints were satisfied through the stress-ratio technique in the linear analysis. Flurry and Schmit (1980) have also solved this problem by using the dual method and the approximation concept and analysis based on the displacement method. The structure was also analyzed using the data provided by Fleury and Schmit and identical results were obtained.

5.1.3. The 72-bar space truss structure

The 72-bar space truss structure, shown in Fig. 3 (see Table 1), is a relatively large size problem. The structure is subjected to two different loading inputs. In the first case, only the node 1 is subjected to a pull load of 22.25 kN (5000 lbf) in the X- and Y-directions and a push load of -22.25 kN (-5000 lbf) in the Z-direction. However, for the second case, all the nodes of 1–4 are subjected to a push load of -22.25 kN (-5000 lbf) in the Z-direction. The number of displacement degrees of freedom is $m = 48$, and the number of the force degrees of freedom is $n = 72$, and hence, the number of the redundancy will be $r = 24$. Without linking together the design variables, the number of the design variables is 72 and the number of the constraints is found to be 152. However, by linking the design variables into 16 groups, the number of the design variables becomes 16, and the associated number of the constraints reduces to 40.

The minimum value of the mass, for both the DM and the FM, was obtained as 172.20 kg (379.615 lbm). The final results are presented in Table 5 and the iteration histories are illustrated in Fig. 13. The required computational time for the FM is significantly lower than the DM, illustrating the efficiency of the FM over the DM for the analysis of large size problems. A closer examination of the results reveals that the nodal displacement constraints at node 1 in the X- and Y-directions for the first load case, and the stress constraints in the elements 1–4 for the second load case are active. The cross-sectional areas in groups 7, 8, 11, 12, 15 and 16 reached their minima in both analyses. The optimum results matches exactly with the solution reported by Flurry and Schmit (1980), who solved the problem using the dual method and the approximation concepts based on the displacement method. Furthermore, the problem was once again solved when the design variables were not linked together. The results using the FM and the DM were found to be almost identical and the computational time for the FM was approximately one half of that required by the DM. The optimum value of the mass was reduced to 131 kg (288.8 lbm), demonstrating that when the symmetry is not imposed on the structure a significantly lower value of the mass can be obtained for the final design. In this case the number of active constraints was 47. The displacement constraints at node 1 in both X- and Y-directions for the first load case, and the stress constraints in the

Table 5
Final design solutions for the cross-sectional areas (mm^2) for the 72-bar space truss

Design variable	Members	DM	FM
1	1–4	100.97	100.97
2	5–12	352.00	352.00
3	13–16	264.77	264.77
4	17,18	367.55	367.55
5	19–22	337.87	337.87
6	23–30	333.61	333.61
7	31–34	64.52	64.516
8	35,36	64.52	64.516
9	37–40	818.32	818.32
10	41–48	330.13	330.13
11	49–52	64.52	64.52
12	53,54	64.52	64.52
13	55–58	1216.90	1216.90
14	59–66	330.52	330.52
15	67–70	64.52	64.52
16	71,72	64.52	64.52
Mass (kg)		172.20	172.20
No. of iterations		556	557
No. of A.C.		9	9
CPU time (s)		274.23	107.10

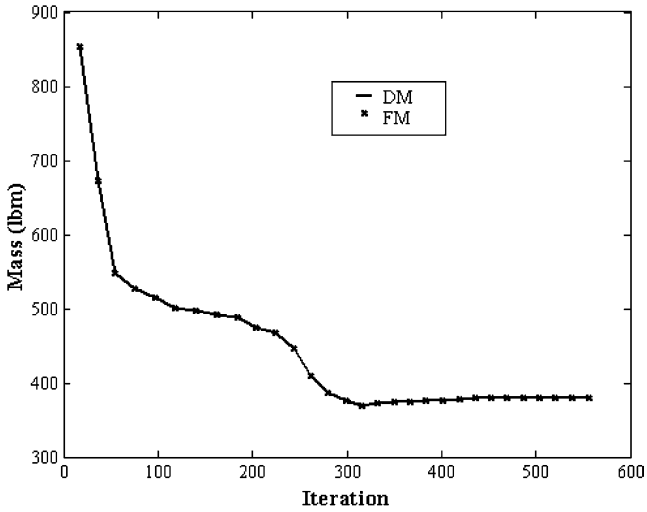

Fig. 13. Iteration histories for the 72-bar space truss structure for both the force and displacement methods with variable linking.

members 1, 2, 4 and 19 for the second load case were found to be active. The cross-sectional areas in the elements 5, 8, 9, 12 to16, 18, 24, 25, 28, 29, 31 to 36, 38, 40, 41, 48 to 54 and 56 were reached to their minima and the iteration histories for this case is illustrated in Fig. 14.

5.1.4. The 10-member frame (two-story and two-bay)

The 10-member frame structure consists of three stories and two bays and illustrated in Fig. 4 (see Table 1). The initial cross-sectional area was set as 16129 mm^2 (25 $in.^2$) that being the same for all the elements. The following empirical relationships were used for the area A, the section modulus S, and the moment of inertia I (Khan, 1984).

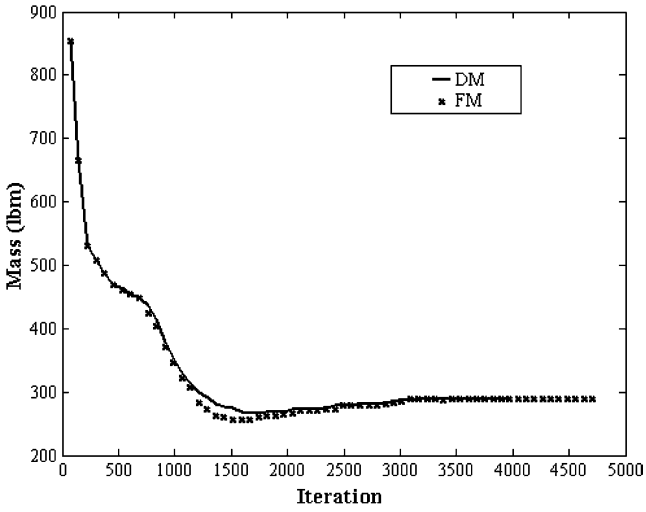

Fig. 14. Iteration histories for the 72-bar space truss structure with no variables linking.

$$\begin{cases} S = 1.6634A^{1.511} \\ I = 4.592A^2 \end{cases} \quad 0 \leqslant A \leqslant 15$$
$$\begin{cases} S = (281.077A^2 + 84100)^{0.5} - 290 \\ I = 4.638A^2 \end{cases} \quad 15 < A \leqslant 44 \tag{37}$$
$$\begin{cases} S = 13.761A - 103.906 \\ I = 256.229A - 2300 \end{cases} \quad 44 < A \leqslant 100$$

where A is the area measured in square inches. The above relationship is stated for a steel section in accordance to the AISC code (AISC, 1978).

A minimum weight of 3307.23 kg (7291.19 lbm) is obtained. Final design solutions for both displacement and force method are tabulated in Table 6. The horizontal displacement constraint at node 4 and the stress constraints on element 6 are identified as active. The horizontal displacement at node 3 is close to being active and the cross-sectional area of the elements 3, 4 and 10 reached their minimum size. The results were compared with those reported in the literature. As an example, Khan (1984) used a displacement based linear analysis with the optimality criterion technique and has obtained a minimum value of the weight 3391.87 kg (7477.79 lbm) with the horizontal displacement of the nodes 3 and 4 being active constraints (no active stress constraint). This problem has also been solved using the CONMIN code and a minimum value of the weight 3969.97 kg (8752.29 lbm) is reported (Vanderplaats, 1973).

The computational time for the force method was significantly lower than that required by the displacement method, again pointing out the efficiency of the force method when applying the force method to the frame-type structures.

5.1.5. The 25-member frame (three-story and three-bay)

The 25-member frame structure, shown in Fig. 5 (see Table 1), corresponds to a three stories and three bays structure. The numerical values of the material properties and the stress limit and the relationship between the cross-sectional area, section modulus and the moment of inertia are all the same as those mentioned in example 5.1.4. The minimum value of the weight is obtained to be 9508.32 kg (20962.26 lbm). The final results are tabulated in Table 7. The horizontal displacement constraints at the nodes 2 and 10, as well as the stress constraints on the elements 1, 2, 3, 5, 9, 12, 14 and 17, are active both in the linear and nonlinear analysis. The cross-sectional areas for the frame elements 6, 11, 13, 15, 18, 20, 24 and 25 reached their

Table 6
Final design solutions for the cross-sectional areas (mm^2) for the 10-member frame structure

Members	DM	FM
1	28387	28387
2	23682	23682
3	3226	3226
4	3226	3226
5	46255	46255
6	10241	10241
7	7236	7236
8	16433	16433
9	16243	16243
10	3226	3226
Mass (kg)	3307.23	3307.23
No. of iterations	620	608
No. of A.C.	5	5
CPU time (s)	63.52	20.60

Table 7
Final design results for the cross-sectional areas (mm^2) for the 25-member frame structure

Members	Linear analysis	
	DM	FM
1	10007	10007
2	7146	7147
3	4233	4233
4	16210	16210
5	20247	20246
6	3226	3226
7	51757	51749
8	14878	14885
9	31429	31429
10	53870	53862
11	64516	64516
12	20581	20581
13	3226	3226
14	19581	19581
15	3226	3226
16	4826	4832
17	13153	13154
18	3226	3226
19	16165	16168
20	3226	3226
21	18751	18754
22	13546	13556
23	46754	46739
24	3226	3226
25	3226	3226
Mass (kg)	9508.32	9508.32
No. of iterations	1849	1665
No. of A.C.	18	18
CPU time (s)	479.93	299.50

minimum size. This problem was also solved by Khan (1984) using the displacement based linear analysis and the optimality criterion technique, having obtained a minimum weight of 10049.77 kg (22155.95 lbm) with just the horizontal displacement at nodes 2 and 11 being active (no active stress constraint). Once again results obtained from the finite element force method, performed in this study, indicate a superior advantage over the ones obtained from the displacement method, as illustrated in Table 7.

5.2. Frequency constraints

In this section the efficiency of the force method in design optimization under frequency constraints have been examined. Three examples shown in Figs. 6–8 (see Table 1) illustrate the proposed procedure and allow the results to be compared with those reported in literatures. Similar to the problems investigated in Section 5.1, all information regarding the material and geometrical characteristics, side constraints and behaviour constraints (natural frequencies) are provided in the relative figures.

5.2.1. 10-Bar planar truss structure with nonstructural lumped masses

The 10-bar planar truss with lumped massed at each of its free nodes is shown in Fig. 6 (see Table 1). Recall that the number of displacement degrees of freedom is $m = 8$, the number of force degrees of

freedom is $n = 10$ and the number of redundancy is $r = 2$. At the initial design, all the cross-sectional areas are 129.03 cm^2 (20 $in.^2$) and the initial mass is 3810.39 kg (8392.94 lbm). This problem was investigated by Venkayya and Tischler (1983), as well as by Grandhi and Venkayya (1988) using the optimality criterion and displacement method. First, the structure was designed with a fundamental frequency of 14 Hz alone, using both the displacement and force methods. A minimum weight of 2637.85 kg (5810.24 lbm) was obtained. The number of iterations required using the FM was lower than that required by the DM. The final results for the cross-sectional areas and fundamental frequency are tabulated in Tables 8 and 9, respectively. Venkayya and Tischler (1983) have reported a minimum mass of 3026.17 kg (6665.577 lbm), where the optimum design was taken as input to compute the specified natural frequency. A fundamental natural frequency of 14.47 Hz was obtained in the present analysis. A simulation carried out using the solution reported in Venkayya and Tischler (1983) as the initial design resulted in a final design, which converged to a lighter solution 2637.85 kg (5810.24 lb obtained before. The current design was based on a consistent mass

Table 8
Final design for the cross-sectional areas (cm^2) for various frequency constraints (Hz) for the 10-bar planar truss structure

Element no.	DM			FM		
	$\omega_1 = 14$	$\omega_2 = 25$	$\omega_1 = 7$ $\omega_2 \geqslant 15$ $\omega_3 \geqslant 20$	$\omega_1 = 14$	$\omega_2 = 25$	$\omega_1 = 7$ $\omega_2 \geqslant 15$ $\omega_3 \geqslant 20$
1	219.909	48.166	38.619	219.903	48.123	38.245
2	47.916	35.852	18.239	47.916	35.832	9.916
3	219.909	48.194	38.252	219.903	48.200	38.619
4	47.916	35.852	9.910	47.916	35.884	18.232
5	0.645	14.800	4.419	0.645	14.826	4.419
6	0.645	7.632	4.200	0.645	7.632	4.194
7	123.626	41.135	24.110	123.626	41.103	20.097
8	123.626	41.142	20.084	123.626	41.181	24.097
9	54.677	13.200	11.452	54.677	13.200	13.890
10	54.677	13.194	13.897	54.677	13.187	11.4516
Mass (kg)	2637.85	871.92	537.01	2637.85	871.92	537.01
No. of iteration	256	1035	637	237	973	705
No. of A.C.	3	1	2	3	1	2
CPU time (s)	10.54	40.81	25.96	7.51	28.70	21.62

Table 9
Final design of natural frequencies (Hz) in different frequency constraints for the 10-bar planar truss structure

Freq. no.	Initial design	DM			FM		
		$\omega_1 = 14$	$\omega_2 = 25$	$\omega_1 = 7$ $\omega_2 \geqslant 15$ $\omega_3 \geqslant 20$	$\omega_1 = 14$	$\omega_2 = 25$	$\omega_1 = 7$ $\omega_2 \geqslant 15$ $\omega_3 \geqslant 20$
1	11.23	14.00	8.01	7.00	14.00	8.01	7.00
2	33.05	18.01	25.00	17.62	18.01	25.00	17.62
3	36.85	29.40	25.00	20.00	29.40	25.00	20.00
4	68.26	34.55	26.68	20.00	34.55	26.68	20.00
5	75.86	49.36	32.83	28.20	49.36	32.83	28.21
6	85.18	53.11	40.92	31.07	53.11	40.94	31.07
7	85.74	85.10	62.52	47.68	85.10	62.52	47.68
8	103.10	90.41	64.79	52.35	90.41	64.78	52.35

matrix. A simulation using a lumped mass matrix resulted in a final design with a minimum mass of 2895.53 kg (6377.82 lbm) suggesting that a lumped mass matrix may have been used by Venkayya and Tischler. To confirm this finding, the optimum result reported in Venkayya and Tischler (1983) was used as input to compute the fundamental natural frequency based on the lumped mass matrix. A fundamental natural frequency of 13.96 Hz was obtained.

To demonstrate the application of the algorithm for designing a structure with other specified natural frequencies, the structure was designed for a second natural frequency of 25 Hz. A minimum mass of 871.92 kg (1920.52 lbm) was obtained. Grandhi and Venkayya (1988) reported a minimum mass of 1018.69 kg (2243.8 lbm). Here, the optimum design was used as input to compute the second natural frequency, resulting in a solution of 25.37 Hz for the second natural frequency. The final results for the cross-sectional areas and the fundamental frequency are given in the Tables 8 and 9.

Finally, the structure was designed under multiple natural frequency constraints given by $\omega_1 = 7$ Hz, $\omega_2 \geqslant 15$ Hz and $\omega_3 \geqslant 20$ Hz. A minimum mass of 537.01 kg (1182.85 lbm) was obtained. Upon closer inspection, the results reveal that the optimum cross-sectional areas for elements 9 and 10 obtained using the FM is different from that using the DM. It is noted that the optimum masses for both the FM and DM are exactly the same and so are the final natural frequencies. It is inferred that, as the optimizer is very sensitive to the output results from the FM and the DM, a small difference causes the optimizer to select a different path. It is interesting to note that, for this case, the number of iterations required by the DM is now lower than that of FM. However, the computational time using the FM is still lower than that of DM. Grandhi and Venkayya (1988) have reported a minimum weight of 594.01 kg (1308.4 lbm). The final cross-sectional areas and natural frequencies are given in Tables 8 and 9. The variation of the optimum mass with the first and second natural frequency limits is shown in Fig. 15. It is observed that, when increasing the fundamental natural frequency limit, the optimum mass increases drastically from 157.95 kg (347.91 lbm) for a fundamental natural frequency limit of 4 Hz to 11448.38 kg (25216.7 lbm) for a fundamental natural frequency limit of 22 Hz. However, a less dramatic change is observed for the second natural frequency limit. The optimum mass increases from 21.26 kg (46.83 lbm) for a second natural frequency limit of 4 Hz to 640.20 kg (1410.14 lbm) for second natural frequency limit of 22 Hz.

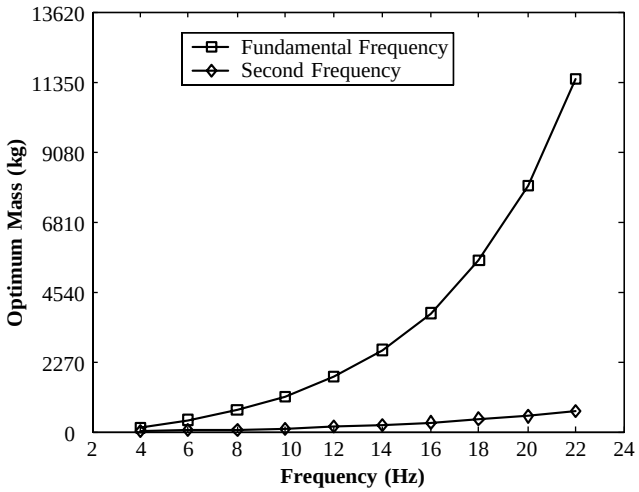

Fig. 15. History of the variation of the optimum mass with respect to the fundamental and second frequencies for the 10-bar planar truss.

5.2.2. 72-Bar space truss structure with nonstructural lumped masses

The 72-bar space truss structure with lumped masses at its four top nodes (nodes 1–4) is shown in Fig. 7 (see Table 1). Recall that the number of displacement degrees of freedom is $m = 48$ and the number of force degrees of freedom is $n = 72$. Therefore, the number of redundancies is $r = 24$. Here the design variables (cross-sectional areas) have been linked into 16 groups so the number of the design variables becomes 16, and the associated number of the constraints reduces to 40.

This problem was investigated by Konzelman and Tabarrok and Konzelman (1986) using the dual method based on approximation concepts for optimization and the finite element method based on displacement method for analysis. Here, the structure was designed for a fundamental frequency of 4 Hz, using both the displacement and the force methods. A minimum mass of 287.09 kg (632.361 lbm) was obtained. For this example, the displacement method was found to be computationally more efficient than the force method approach. The reason is that SVD technique used to develop the compatibility is not a cheap technique and when the number of redundancy increases (as this example), generating the compatibility matrix using SVD becomes computationally expensive. Thus, in optimal design problems with frequency constraints, the analysis of not highly redundant structures using the force method is not necessarily more efficient than the DM. The final results for the cross-sectional areas and frequencies are given in Tables 10 and 11 and they are in excellent agreement with those reported by Konzelman (1986) who reported a minimum mass of 287.09 kg (632.36 lbm). Due to the symmetry imposed by the structural geometry and the linking scheme, the eigenvalue corresponding to the fundamental mode of vibration is a repeated eigenvalue of multiplicity two. This means that in the initial and optimum design, the first and second modes of vibration have the same natural frequencies. Thus, a small change or deviation in the geometry of the structure can switch the mode of vibration from first to the second mode.

Table 10
Final design for the cross-sectional areas (cm^2) for the various frequency constraints (Hz) for the 72-bar space truss structure

Element no.	DM		FM	
	$\omega_1 = 4$	$\omega_1 = 4$ $\omega_3 \geqslant 6$	$\omega_1 = 4$	$\omega_1 = 4$ $\omega_3 \geqslant 6$
1–4	4.717	3.499	4.717	3.499
5–12	5.514	7.932	5.514	7.932
13–16	0.645	0.645	0.645	0.645
17–18	0.645	0.645	0.645	0.645
19–22	11.750	8.056	11.750	8.056
23–30	5.573	8.011	5.573	8.011
31–34	0.645	0.645	0.645	0.645
35–36	0.645	0.645	0.645	0.645
37–40	18.950	12.812	18.950	12.812
41–48	5.607	8.061	5.607	8.061
49–52	0.645	0.645	0.645	0.645
53–54	0.645	0.645	0.645	0.645
55–58	25.935	17.279	25.934	17.279
59–66	5.628	8.088	5.628	8.088
67–70	0.645	0.645	0.645	0.645
71–72	0.645	0.645	0.645	0.645
Mass (kg)	287.092	327.605	287.092	327.605
No. of iteration	544	379	510	379
No. of A.C.	9	10	9	10
CPU time (s)	283.78	200.37	302.96	227.62

Table 11
Final design results for the natural frequencies (Hz) with different sets of frequency constraints for the 72-bar space truss structure

Freq. no.	Initial design	DM		FM	
		$\omega_1 = 4$	$\omega_1 = 4$ $\omega_3 \geqslant 6$	$\omega_1 = 4$	$\omega_1 = 4$ $\omega_3 \geqslant 6$
1	3.113	4.000	4.000	4.000	4.000
2	3.113	4.000	4.000	4.000	4.000
3	5.374	5.001	6.000	5.001	6.000
4	9.425	6.505	6.247	6.505	6.247
5	13.189	8.595	9.074	8.595	9.074

It is noted that when the eigenvalues are repeated, the structures becomes extremely sensitive to any change in design variables. Usually the natural frequencies of the first few modes are important and to separate these eigenvalues in the optimum design, the frequency constraints of the first few modes have to be separated. In this example, due to the intrinsic nature of symmetry in the structure, any attempt to separate the fundamental and second natural frequencies in the optimum design failed. To quantify the performance of the algorithm for multiple frequency constraint problems, the structure was designed using the displacement methods and force method for $\omega_1 = 4$ Hz and $\omega_3 \geqslant 6$ Hz. A minimum mass of 327.605 kg (721.597 lbm) was obtained. The results are given in Tables 10 and 11.

5.2.3. Member frame (two-story and one-bay) with nonstructural distributed mass

The 6-member frame is illustrated in Fig. 8 (see Table 1). This problem has been studied by Khan and Willmert (1981) and McGee and Phan (1991) using the optimality criterion method combined with the finite element method based on the displacement formulation.

The moment of inertia, I is empirically related to the area, A, by the following expressions (Khan and Willmert, 1981; McGee and Phan, 1991):

$$\begin{aligned} I &= 4.6248A^2 \quad 0 \leqslant A \leqslant 44 \\ I &= 256A - 2300 \quad 44 < A \leqslant 88.2813 \end{aligned} \tag{38}$$

where A is the area measured in square inches. At the initial design, all the cross-sectional areas are equal to193.55 cm^2 (30 $in.^2$) with an initial mass of 5034 kg (11088 lbm). First, the structure was optimized using both the displacement and force method giving a fundamental natural frequency of 78.5 rad/s. A minimum mass of 4272.32 kg (9410.39 lbm) was obtained. It is interesting to note that the final design variables (cross-sectional areas) are different in the displacement method and forced method solutions, suggesting that the optimum solution is not unique. However, the final natural frequencies are the same. It is noted that although the optimum results obtained using the force method and displacement method are different; they resulted in the same optimum mass and same final natural frequency. Therefore, both are optimum solutions. The results are given in Tables 12 and 13. Khan and Willmert (1981) and McGee and Phan (1991) report a minimum weight of 4341 kg (9561 lbm) and 4456 kg (9815 lbm), respectively. To verify that the optimality criterion employed by Khan and Willmert (1981) and McGee and Phan (1991) may have produced a local minimum, another simulation was performed, starting with the solution reported in Khan and Willmert (1981) and McGee and Phan (1991). This solution process resulted in a design change and converged to a lighter solution of 4272.32 kg (9410.39 lbm). Thus, it is confirmed that the solution in Khan and Willmert (1981) and McGee and Phan, 1991 does not represent a local minimum.

The structure was again designed using multiple natural frequency constraints of $\omega_1 = 78.5$ rad/s and $\omega_2 \geqslant 180$ rad/s. Surprisingly, the optimum mass of 4365.56 kg (9615.78 lbm) using force method and 4418.46 kg (9732.3 lbm) using displacement method was obtained. As explained before, this specific problem is path dependent and the slightly difference in output results from analyzers (force method and

Table 12
Final design for the cross-sectional areas (cm^2) for different sets of frequency constraints (rad/s) for the 6-member frame

Element no.	DM		FM	
	$\omega_1 = 78.5$	$\omega_1 = 78.5, \omega_2 \geqslant 180$	$\omega_1 = 78.5$	$\omega_1 = 78.5, \omega_2 \geqslant 180$
1	215.867	120.556	51.088	206.289
2	51.088	141.802	215.551	62.746
3	51.088	283.870	365.982	138.767
4	367.203	227.761	51.088	297.876
5	51.088	51.088	51.088	51.088
6	253.087	228.549	253.799	256.361
Mass (kg)	4272.35	4418.46	4272.32	4365.56
No. of Iteration	320	726	258	246
No. of A.C.	4	2	4	3
CPU time (s)	15.31	34.29	11.76	11.21

Table 13
Final design results for the natural frequencies (rad/s) for different sets of frequency constraints for the 6-member frame

Freq. no.	Initial design	DM		FM	
		$\omega_1 = 78.5$	$\omega_1 = 78.5, \omega_2 \geqslant 180$	$\omega_1 = 4$	$\omega_1 = 78.5, \omega_2 \geqslant 180$
1	69.044	78.500	78.500	78.500	78.500
2	286.840	146.670	220.806	146.668	180.000
3	380.324	268.399	436.420	268.350	371.289
4	476.168	350.723	486.975	350.667	418.804
5	499.720	465.900	540.125	465.780	485.897

displacement method) may have caused a different optimum solution. Investigating the final natural frequencies obtained from the displacement method and the force method, it was revealed that in the force method, the inequality constraint is active in the optimum solution, and this is not observed in the solution from the displacement method. This is the reason for a lighter mass obtained using the force method. For this case, the force method performed better computationally than the displacement method. It can be inferred that for frequency constraint problems, the computational time totally depends on the iteration number.

6. Conclusion

A structural optimization algorithm, using integrated force formulation technique, has been developed to minimize the mass of truss and frame type structures under the stress, displacement and frequency constraints. The required compatibility matrix in the formulation has been derived directly by utilizing a displacement–deformation relationship and the Single Value Decomposition Technique. Moreover, the Sequential Quadratic Programming method has been adopted to optimize the truss and frame structures.

The main objective of this study is to investigate the relative performance of the force and displacement methods in the design and optimization of different planar and space structures with the stress–displacement and frequency constraints. It is found that the optimization technique that is based on the force method is computationally far more efficient than the displacement method for structural design optimization under stress–displacement constraints. It is also concluded that, in some problems with multiple frequency constraints, the optimization based on the force method may result in a lighter design. It is noted that this is not a general case, and they are specific results for the examples presented.

Last but not least, from the results obtained from eight different benchmark examples, it is demonstrated that the Sequential Quadratic Programming method could result into a lighter optimal design of space structures when compared to the conventionally used optimality criterion techniques. The proposed methodology has proved to be extremely efficient in the analysis and optimization of the truss and frame type space structures.

Acknowledgment

Support by the Natural Sciences and Engineering Research Council (NSERC) of Canada is gratefully acknowledged.

References

AISC, 1978. Specification for the Design, Fabrications and Erection of Structural Steel for Buildings. American Institute of Steel Constructions, Chicago IL, USA.

Canfield, R.A., Grandhi, R.V., Venkayya, V.B., 1988. Optimum design of structures with multiple constraints. AIAA Journal 26, 78–85.

Coleman, T., Branch, M.A., Grace, A., 1999. Optimization toolbox for use with Matlab. User's Guides, Version 2. The MathWorks Inc.

Flurry, C., Schmit Jr., L.A., 1980. Dual methods and approximation concepts in structural synthesis. NASA CR-3226.

Golub, G.H., Van Loan, C.F., 1996. Matrix Computations, third ed. The Johns Hopkins University Press, Baltimore and London.

Grandhi, R.V., Venkayya, V.B., 1988. Structural optimization with frequency constraints. AIAA Journal 26, 858–866.

Haftka, R.T., Gurdal, Z., 1992. Elements of Structural Optimization, third ed. Kluwer Academic Publishers.

Khan, M.R., Willmert, K.D., 1981. An efficient optimality criterion method for natural frequency constrained structures. Computers & Structures 14, 501–507.

Khan, M.R., 1984. Optimality criterion techniques applied to frames having general cross-sectional relationships. AIAA Journal 22 (5), 669–676.

Khot, N.S., Kamat, M.P., 1985. Minimum weight design of truss structures with geometric nonlinear behavior. AIAA Journal 23, 139–144.

Khot, N.S., 1984. Optimization of structures with multiple frequency constraints. Computers & Structures 20 (5), 869–876.

Konzelman, C.J., 1986. Dual Methods and Approximation Concepts for Structural Optimization, M.A.Sc thesis, Department of Mechanical engineering, University of Toronto.

McGee, O.C., Phan, K.F., 1991. A robust optimality criteria procedure for cross-sectional optimization of frame structures with multiple frequency limits. Computers & Structures 38, 485–500.

Mohr, G.A., 1992. Finite Elements for Solids, Fluids, and Optimization. Oxford University Press.

Mohr, G.A., 1994. Finite element optimization of structures-I. Computers & Structures 53, 1217–1220.

Patnaik, S.N., Joseph, K.T., 1986. Generation of the compatibility matrix in the integrated force method. Computer Methods in Applied Mechanics and Engineering 55, 239–257.

Patnaik, S.N., Berke, L., Gallagher, R.H., 1991. Integrated force method versus displacement method for finite element analysis. Computers & Structures 38 (4), 377–407.

Patnaik, S.N., 1986. The integrated force method verses the standard force method. Computers & Structures 22 (2), 151–163.

Powell, M.J.D., 1978. A fast algorithm for nonlinearly constrained optimization calculations. In: Watson, G.A. (Ed.), Lecture Notes in Mathematics and Numerical Analysis. Springer-Verlag, p. 630.

Robinson, J., 1965. Automatic selection of redundancies in the matrix force method: the rank technique. Canadian Aero Space Journal 11, 9–12.

Saka, M.P., Ulker, M., 1992. Optimum design of geometrically nonlinear space trusses. Computers & Structures 42, 289–299.

Saka, M.P., 1984. Optimum design of space trusses with buckling constraints. Proceeding of the Third International Conference on Space Structures. University of Surrey, Guildford, UK.

Sedaghati, R., Tabarrok, B., 2000. Optimum design of truss structures undergoing large deflections subject to a system stability constraint. International Journal for Numerical Methods in Engineering 48 (3), 421–434.

Timoshenko, S., 1953. History of Strength of Material. McGraw-Hill, New York.

Vanderplaats, G.N., 1973. CONMIN- A FORTRAN program for constrained function minimization. User's Manual, NASA TMX-G2.

Venkayya, V.B., Tischler, V.A., 1983. Optimization of Structures with Frequency Constraints. Computer Methods for Nonlinear Solids and Structural Mechanics ASME AMD-54, 239–259.

Venkayya, V.B., 1978. Structural optimization: a review and some recommendations. International Journal for Numerical Methods in Engineering 13, 203–228.